Heliyon 11 (2025) e41919

Contents lists available at ScienceDirect

Heliyon

journal homepage: www.cell.com/heliyon

Research article

Ultrasound stimulated perfluorobutane microbubbles cavitation enhanced the therapeutic effect of colchicine in rats with acute gouty arthritis

Ji-cheng Zhang [a,1], Bo Gou [a,1], Tian-rui Wang [a], Wan-tai Dang [b], Yan-hui Li [a], Wen Wen [a,**], Jian Liu [a,*]

[a] Department of Ultrasound, Clinical Medical College and the First Affiliated Hospital of Chengdu Medical College, Chengdu, China
[b] Department of Rheumatic Immunology, Clinical Medical College and the First Affiliated Hospital of Chengdu Medical College, Chengdu, China

ARTICLE INFO

Keywords:
Ultrasound stimulated microbubbles
Cavitation
Acute gouty arthritis
Colchicine

ABSTRACT

Objective: This study aimed to explore whether cavitation generated by ultrasound-stimulated microbubbles (USMB) can enhance the therapeutic efficacy of colchicine and diminish its gastrointestinal side effects in rats with acute gouty arthritis (AGA).

Materials and methods: The rat AGA model was established by injection of Monosodium urate (MSU) crystals. The rats were randomly divided into 6 groups (A: control group, B: model control group, C: cavitation group, D: high dose colchicine group, E: cavitation + low dose colchicine group, F: cavitation + high dose colchicine group) according to whether they were given cavitation and different doses of colchicine. The effect of cavitation on blood perfusion was analyzed by comparing contrast-enhanced ultrasound (CEUS) and the area under the curve (AUC) of CEUS with the ankle joint of right hind limb. The AGA symptoms were assessed by referring to the degree of ankle joint swelling within 24 h and the gait score. The infiltration of neutrophils was determined using the hematoxylin-eosin (HE) staining method. For the evaluation of vascular inflammation and dilation, plasma interleukin-1β (IL-1β) and endothelial nitric oxide synthase (eNOS) served as the key indicators. Besides, the severity of gastrointestinal adverse reactions is determined by analyzing the gastrointestinal reaction scores.

Results: When compared with groups A, B, and D, the AUC was markedly higher in groups C, E, and F (all $P < 0.05$). In groups E and F, the degree of ankle swelling, gait scores, and the level of plasma IL-1β in AGA rats were lower, while the concentration of plasma eNOS was higher compared to the group D (all $P < 0.05$). HE staining findings demonstrated that the integration of cavitation and colchicine played a positive role in reducing neutrophil infiltration in the ankle joint synovium and mitigating the gastrointestinal reaction score in AGA rats. In contrast to groups D, E, and F that were given colchicine, group E had a substantially lower gastrointestinal reaction score, with statistically significant differences observed in pairwise comparisons (all $P < 0.05$).

Conclusion: In rats with AGA, cavitation generated by USMB exerted a remarkable effect on augmenting the blood perfusion of the ankle joint. This, in turn, not only amplified the anti-gout

* Corresponding author.
** Corresponding author.
E-mail addresses: 252884218@qq.com (W. Wen), drliujian0524@163.com (J. Liu).
[1] These authors contributed equally:Ji-cheng Zhang and Bo Gou.

https://doi.org/10.1016/j.heliyon.2025.e41919
Received 27 May 2024; Received in revised form 31 December 2024; Accepted 10 January 2025
Available online 11 January 2025

efficacy of colchicine but also reduced the dosage of colchicine. Concurrently, it effectively mitigated the associated gastrointestinal side effects.

1. Introduction

Gouty arthritis (GA), ranking among the prevalent forms of inflammatory arthritis, is distinguished by abnormally high levels of serum uric acid. This elevation of serum uric acid will prompt the deposition of monosodium urate crystals within the joints [1], thereby causing excruciating joint pain in patients. Patients with acute gouty arthritis (AGA) usually suffer from intense pain and severe discomfort during episodes. Notably, the incidence of AGA has been on a steady climb in recent years, showing a disconcerting trend of affecting younger populations [2]. In clinical practice, the treatment of AGA typically involves non-steroidal anti-inflammatory drugs, colchicine, glucocorticoids, and other symptomatic interventions. Among these options, colchicine has emerged as a highly efficacious and commonly adopted therapeutic strategy. However, the inherent toxicity of colchicine also limits its further application in clinical practice. For instance, after treatment with colchicine, patients may experience serious complications, including diarrhea, vomiting, and bone marrow suppression [3]. These adverse reactions have a detrimental impact on the patient's quality of life and prognosis Compelling clinical evidence has established a direct correlation between the dose of colchicine administered and the occurrence of adverse reactions in patients. Given this, there is an urgent need to explore alternative drug regimens that can achieve high therapeutic efficacy with minimal dosing, thereby reducing the potential harm to patients and improving overall treatment outcomes.

Ultrasound-stimulated microbubbles (USMB) represent an innovative technological approach. This method involves the introduction of contrast agent microbubbles (taking sulfur hexafluoride microbubbles and perfluorobutane microbubbles as examples) into the human body during ultrasonic irradiation. Adjusting the relevant physical parameters of ultrasound allows these microbubbles to induce cavitation, which in turn offers supportive treatment for a range of conditions, including cancer therapy and gene therapy [4,5]. In recent years, an increasing number of studies have found that USMB can trigger stable cavitation by modifying the relevant parameters of ultrasound diagnostic equipment [6,7]. Such cavitation plays a significant role in temporarily heightening local blood perfusion and promoting the osmotic release of drugs in the local tissues, facilitating better therapeutic outcomes. This technology has been widely used in the basic research of tumor chemotherapy and can enhance the effect of tumor chemotherapy [8,9]. Depending on the energy generated, the cavitation effect can be categorized into transient cavitation, characterized by high energy, and steady-state cavitation, characterized by low energy. Previous studies on the ultrasonic cavitation effect have predominantly focused on transient cavitation. The transient emergence of infinitesimal perforations on the cell membrane interface substantially augments the penetrability of membrane, consequentially optimizing the delivery proficiency of plasmids and drugs. In addition, the immense energy instantaneously released during cavitation events exhibits the capacity to dismantle microvessels within tumor tissues, thereby making it a highly attractive research focus in both gene therapy and oncology treatment domains [10,11]. Perfluorobutane microspheres are relatively stable, and are not easily broken during cavitation irradiation, and are theoretically easy to produce steady-state cavitation.

Consequently, the objective of our research was to investigate whether the application of USMB with perfluorobutane microspheres could enhance the therapeutic efficacy of colchicine. Simultaneously, we aimed to ascertain if it was possible to cut down the dosage of colchicine required, all while curtailing the occurrence and severity of its associated gastrointestinal side effects to the greatest extent.

2. Materials and methods

2.1. Laboratory animal

A total of 30 adult male Sprague Dawley rats, with an approximate body weight ranging from 230 to 250 g each, were supplied by Dashuo Co., LTD. The ethical clearance for the animal experimentation involved in this study was granted by the Ethics Committee of the First Affiliated Hospital of Chengdu Medical College (No.2023-028). All experimental procedures were executed in strict adherence to the ARRIVE guidelines formulated specifically for animal research.

2.2. Experimental equipments and drug reagents

Colchicine (purchased from McLean, USA); Monosodium urate (MSU) crystal (Sigma Co., USA); VINNO 70 G86 ultrasonic cavitation diagnostic instrument (produced in 2022, VINNO technology Co., LTD. China); Perfluorobutane microspheres contrast agent (Sonazoid; GE Healthcare, Norway); ELISA kit of IL-1B and eNOS (FBIO, China); Inhalation anesthetic Isoflurane (Rayward, China); The original solution was prepared by diluting 16 μL perfluorobutane microspheres with 5 mL normal saline. Sonazoid: normal saline at a concentration 1:1 was used as a contrast agent, while a concentration of 1:9 was used for cavitation. Colchicine was dissolved in normal saline to yield low concentration (2 mg/ml) and high concentration solutions (4 mg/ml). MSU crystals were dissolved in normal saline to obtain a concentration of 50 mg/ml sodium urate crystal suspension. Hereafter referred to as MSU.

2.3. Modeling and grouping

Anesthesia: the rats were placed in the induction cage of a small animal anesthesia machine and anesthetized with 3 % isoflurane at

a flow rate of 1L/min. When the upper and lower limbs of rats were pulled, if the muscle tone was reduced, it was indicated that the anesthesia was successfully induced. After successful anesthesia, the rats were removed, and the maintenance mask was closed tightly to the mouth and nose of the rats, and the rats were anesthetized with 3 % isoflurane at 0.5L/min. Drawing upon the traditional modeling delineated by Coderre et al. [12], after the rats were anesthetized, the MSU solution, prepared at a concentration of 50 mg/ml, was administered posterolaterally into the articular cavity of the ankle joint of right hind limb, with a total volume of 100 μL.

Upon completion of the modeling process, the rats were randomly sorted into six distinct groups, with five rats in each group. The specific groupings were configured as follows: Group A served as the control group, wherein rats received only a standard volume of normal saline injection directly into the ankle joint, acting as a baseline for comparison. Group B was established as the AGA model group, designed to mimic the disease state under investigation. Group C was identified as the cavitation group. In this cohort, rats diagnosed with AGA were subjected solely to cavitating irradiation on their joints, allowing for the assessment of the independent effect of cavitation. Group D was labeled as the high-dose colchicine group. Rats belonging to this group, all afflicted with AGA, underwent treatment with a high-concentration (4 mg/ml) colchicine solution, without any concurrent cavitation therapy, aiming to evaluate the impact of high-dose drug treatment alone. Group E was designated as the cavitation + low-dose colchicine group. Here, rats with AGA received a low-concentration colchicine (2 mg/ml) regimen in combination with cavitation treatment, probing the potential synergistic effect of the two interventions. Group F was termed the cavitation + high-dose colchicine group, signifying that rats in this group received high-dose colchicine therapy along with cavitation treatment, further exploring the combined influence of these two therapeutic approaches.

2.4. Method of administration

Groups D, E, and F were given colchicine solution 1h after MSU intragastrically. These three groups were given colchicine solution at a dose of 4 ml/kg by gavage.

2.5. CEUS and cavitation method

In the context of contrast-enhanced ultrasound (CEUS) imaging, the X4-12L linear array probe was utilized for the procedure. Concurrently, the VINNO 70 G86 ultrasonic diagnostic device was calibrated to engage the contrast mode, facilitating the acquisition of ankle arthrographic images both preceding and subsequent to the cavitation process. Prior to the cavitation procedure, the initial CEUS examination was performed approximately 7 h post-injection of MSU, following the intravenous injection of 0.2 ml of contrast agent solution into the tail veins of the rats. Subsequently, the second CEUS was conducted approximately 30 min after cavitation, at which point the microbubbles in systemic circulation had substantially cleared, thereby minimizing interference with the subsequent CEUS assessment. Tubes of rats' tail vein were flushed with 0.5 mL 0.9 % normal saline after each CEUS. The area under the curve (AUC) is a parameter of time-intensive-curve in CEUS. And AUC is the integral value of the contrast intensity at each time point to the contrast time, reflecting the cumulative perfusion intensity during the whole contrast period.

Cavitation: The cavitation procedure was executed utilizing the X4-12L linear array probe under VFlash mode. Concurrently, a cavitation solution of 1 ml was administered via slow and uniform injection into the tail vein of the rats over a period of 10 min, ensuring the maintenance of contrast agent microbubbles without interruption. Post-administration of the cavitation solution, the rats' ankles were positioned within the region of interest (ROI) and allowed to remain undisturbed for a duration of 10 min. The ROI was the region where the ultrasound focused during cavitation irradiation. The size of ROI can be adjusted so that the rat ankle joint can be completely covered. A multitude of parameters, acoustic power, pulse length, pulse repetition frequency, pulse duration, and encompassing center frequency, were meticulously optimized to establish the most favorable conditions for the experiment. In this study, we adjusted the probe frequency of cavitation to 3 MHz, the pulse repetition rate to 1000Hz, and the pulse length to 10.5 cycles.

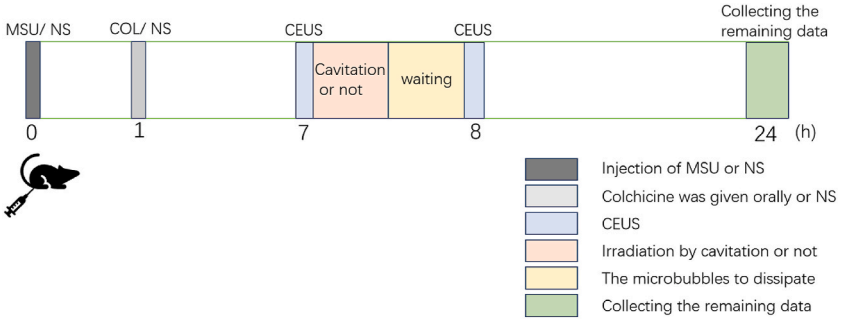

Fig. 1. Brief experimental procedure.
Approximately 1 h subsequent to the injection of MSU, colchicine solution was administered to rats in Groups D, E, and F. Around 7 and 8 h post the MSU injection, ankle joint CEUS examinations were carried out for all the experimental rats. Following the initial data comparison, cavitation irradiation was applied to the ankle joints of rats belonging to Groups C, E, and F. At approximately 24 h after the start of the experiment, all the rats were euthanized, and the remaining data were then collected for further analysis. MSU: Monosodium urate, CEUS: contrast-enhanced ultrasound, COL: colchicine, NS: normal saline solution.

These refinements were strategically implemented to attain a mechanical index (MI) of approximately 0.28, which is conducive to the induction of cavitation (Fig. 1).

2.6. Test indicators

2.6.1. AUC values of rat ankle joints

CEUS was performed twice on the rat ankle joint at 7h (before the cavitation) and 8h (after the cavitation) after the injection of MSU, and the dynamic images of two CEUS were obtained (continuous storage for 60s each time). The ROI was delineated along the edge of the rat ankle joint using the analysis software of VINNO 70 G86 ultrasound diagnostic instrument, and the 60s dynamic images were analyzed. The AUC values of two CEUS in the rat ankle were obtained.

2.6.2. Ankle joint swelling degree

In each rat, a demarcation was made at the center of the ankle joint. The circumference of the marked area at the ankle joint was measured using a vernier caliper before the injection of MSU and again at 24 h post-injection. The degree of ankle joint swelling was quantified using the following formula:=(b-a/a). where a represents the original circumference of the ankle joint, and b denotes the circumference of the ankle joint measured 24 h post MSU injection.

2.6.3. Gait score

The rats were transferred from their original cages to plexiglass enclosures approximately 24 h subsequent to the MSU. During this interval, the right pedal extremity of each rat was subjected to a 5-min observational period to assess any alterations in gait or the presence of lameness indicative of the model's efficacy. The severity was graded on a scale as follows: 0 denoting a normal gait; 1 indicating slight claudication, characterized by a pronounced exaggeration in the flexion of the affected limb; 2 representing moderate claudication, where the affected limb made only fleeting contact with the ground; and 3 signifying severe claudication, with the affected limb being completely elevated, resulting in the rat ambulating on three limbs [12]. In instances of ambiguity, the scoring was conducted independently by two investigators, and the outcomes were subsequently averaged to ensure objectivity and reliability in the assessment.

2.6.4. Pathological examination

The right hind limb ankle joints of a cohort of 30 rats were subjected to fixation using a 10 % formaldehyde solution and subsequent decalcification with a proprietary decalcifying agent. Following these procedures, the specimens were embedded in paraffin, sectioned into 2-μm-thick coronal slices, and subsequently processed for hematoxylin-eosin (HE) staining to facilitate histological examination.

2.6.5. Detection of IL-1β and eNOS

Blood samples were harvested from the rat tail vein over a 24-h period following the injection of MSU. Subsequently, the rat serum was isolated under low-temperature conditions at 3000 revolutions per minute using a low-speed refrigerated centrifuge for a duration of 15 min. The expression levels of serum inflammatory markers, IL-1βand eNOS, were ascertained in accordance with the manufacturers' protocols.

2.6.6. Gastrointestinal reaction observation

The fecal output of the rats was meticulously monitored within a 24-h period following the induction of the model to assess gastrointestinal responses. The degree of fecal molding was quantified using a standardized scoring system, where 0 indicated the presence of fecal molding with relative dryness, 1 denoted fecal molding accompanied by relative wetness, and 2 signified the absence of fecal form [13]. In instances where multiple defecations were observed, the highest score was recorded. The scoring was conducted

Fig. 2. Gastrointestinal response score in rats.
The gastrointestinal reaction score of rats: ① the stool was granular and dry, and scored 0; ② The stool was basically formed and moist, and 1 point was scored; ③ The feces were not formed and the perianal hair of rats was moist and colored, and scored 2 points.

independently by two researchers, and the results were averaged to ensure the accuracy and reliability of the data (Fig. 2).

2.7. Statistical analysis

The determination of sample size was executed utilizing the PASS11.0 software. Subsequent data analysis was performed employing the SPSS 24.0 software, wherein group differences adhering to normal distribution and homogeneity of variance were assessed via one-way ANOVA. For group comparisons that deviated from normal distribution and variance homogeneity, the Kruskal-Wallis H test was deployed. In cases where normal distribution was met but variance homogeneity was not, Tamhane's T2 test was applied. Statistical significance was ascertained at the threshold of $P < 0.05$.

3. Results

3.1. MSU induced AGA in rats

Following the administration of MSU, the right hind limb ankle joints of the rats exhibited a gradual onset of inflammatory signs, marked by the appearance of a crimson hue, swelling, and an elevated temperature, which intensified over the course of 8–12 h. At approximately 24 h post-MSU injection, the ankle joint swelling peaked, and concurrently, the rats' gait underwent a progressive transformation, notably adopting a three-legged locomotion pattern, thereby confirming the efficacy of the model. The modeling success rate was 100 %. The pertinent experimental data are presented in Table 1.

3.2. Effects of USMB increased blood perfusion in the ankle joint in AGA

There was no significant difference in AUC between groups at 7h (before cavitation) (all $P > 0.05$). The AUC values of groups C, E and F at 8 h (after cavitation treatment) were significantly higher than those at 7h (all $P < 0.05$). AUC values between groups at 8h: The AUC value of group C, E and F was higher than that of group A, and the difference was statistically significant (all $P < 0.05$). The AUC value of group C, E and F was higher than that of group B, and the difference was statistically significant (all $P < 0.05$). There was no significant difference between the other groups (all $P > 0.05$). Comparison of ankle CEUS in each group: the blood perfusion of groups C, E and F increased significantly after cavitation. The ankle arthrography and corresponding AUC values of each group are shown in Table 1, Fig. 3 and 4(A–F).

3.3. Effects of USMB combined with colchicine on ankle symptoms in AGA

The swelling degree of ankle joint in group B, C, D, E and F was higher than that in group A (all $P < 0.05$). After treatment, the degree of ankle swelling in groups D, E and F decreased, which were significantly lower than those in group B and group C (all $P < 0.05$). However, after receiving USMB combined with high dose colchicine treatment, the degree of ankle swelling in group F was significantly lower than that in groups D and E ($P < 0.05$). (Fig. 5: A-F); Compared with group B, C, D and E, the gait score of group A was lower ($P < 0.05$). The gait scores of groups D, E and F were lower than those of groups B and C ($P < 0.05$). However, after the treatment with USMB combined with high dose colchicine, the gait score in group F decreased significantly, which was lower than that in groups D and E, and the differences were statistically significant (all $P < 0.05$). These results suggested that USMB combined with colchicine is more effective than either treatment. (Tables 1 and 2).

3.4. Effects of USMB combined with colchicine on plasma IL-1β and eNOS concentrations in AGA

At 24 h after injection of MSU crystal suspension, the plasma IL-1β concentration in group B and C was higher than that in group A ($P < 0.05$). The plasma IL-1β concentration in groups D, E and F was also lower than that in group B and C($P < 0.05$). The plasma eNOS concentration in group B, C, E and F was higher than that in group A ($P < 0.05$). The plasma eNOS concentration in group C, E and F was higher than that in group B ($P < 0.05$). The plasma eNOS concentration in group D was lower than that in groups E and F ($P <$

Table 1
Comparison of AUC values at 7 h and 8 h and measurement data at 24 h among groups($\overline{x} \pm s$).

Group	AUC of Pre-Cavitation	AUC of Post-Cavitation	ankle joint swelling degree(%)	IL-1 (pmol/ml)	eNOS (pmol/ml)
A	108.78 ± 7.41	107.98 ± 6.04	0.59 ± 0.34	3.01 ± 0.63	267.64 ± 71.51
B	103.58 ± 5.66	109.10 ± 9.23	15.48 ± 0.90[a]	24.91 ± 9.07[a]	627.27 ± 230.03[a]
C	102.14 ± 5.55	216.74 ± 27.08[ab]	15.26 ± 1.11[a]	32.11 ± 7.85[a]	963.41 ± 118.13[ab]
D	113.44 ± 4.44	107.20 ± 6.07[c]	3.93 ± 1.02[abc]	9.20 ± 1.95[bc]	365.16 ± 130.09[bc]
E	104.82 ± 7.04	190.22 ± 50.04[abd]	3.51 ± 1.63[abc]	10.30 ± 2.90[bc]	903.50 ± 319.00[abd]
F	103.74 ± 6.04	188.04 ± 26.90[abd]	1.33 ± 0.61[abcde]	6.43 ± 2.13[bc]	761.75 ± 325.96[abd]
F	1.940	14.833	180.463	19.710	6.512
P	0.125	<0.001	<0.001	<0.001	<0.001

Compared with group A, [a]$P < 0.05$; Compared with group B, [b]$P < 0.05$; Compared with group C, [c]$P < 0.05$; Compared with group D, [d]$P < 0.05$; Compared with group E, [e]$P < 0.05$.

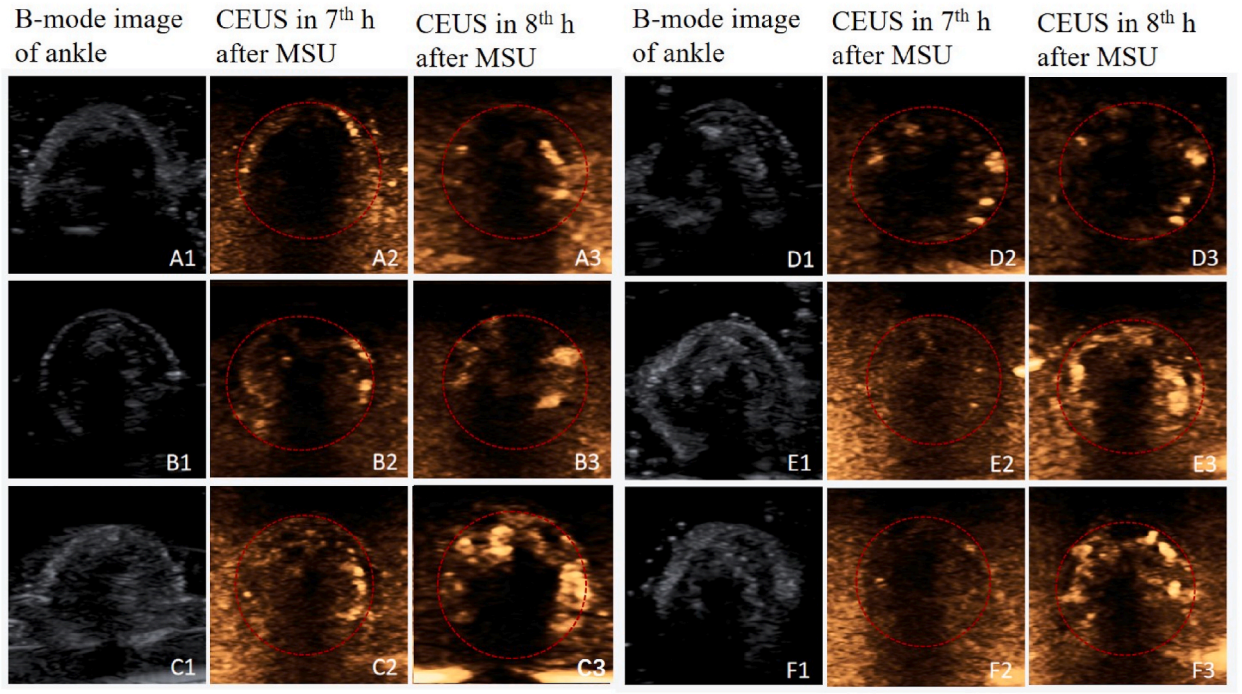

Fig. 3. Contrast enhanced ultrasound (CEUS) images before and after cavitation: A: control group, B: model control group, C: cavitation group, D: high dose colchicine group, E: cavitation + low dose colchicine group, F: cavitation + high dose colchicine group. A1, A2, and A3 represent the two-dimensional images of the ankle joint in group A, the CEUS of the ankle joint in group A at 7 h, the CEUS of the ankle joint in group A at 8 h, and so on.

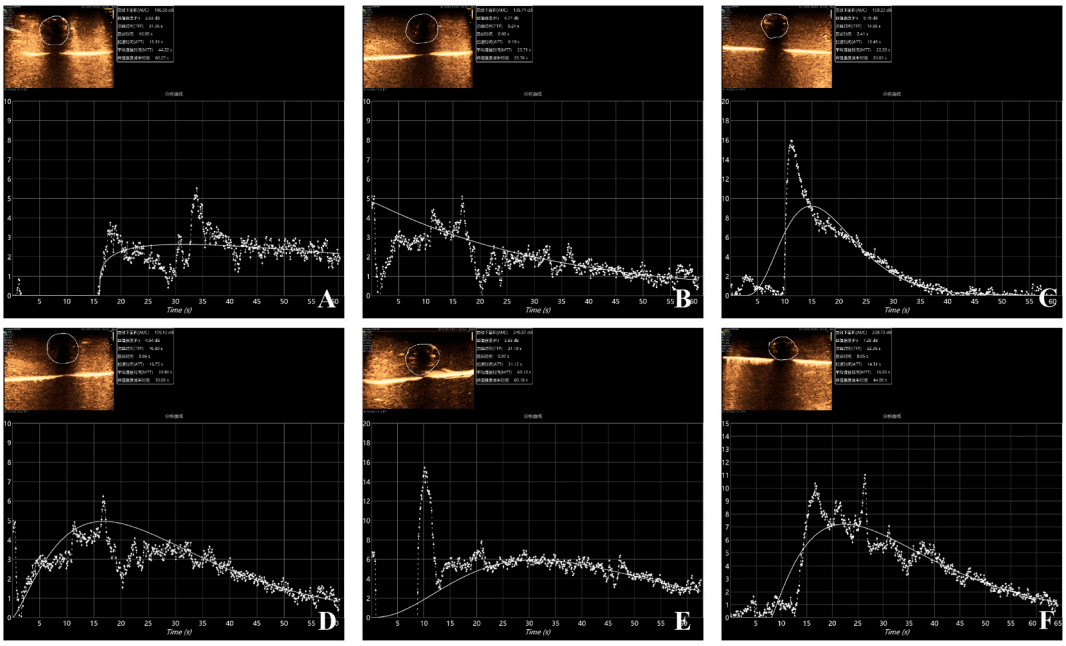

Fig. 4. Area under curve analysis: AUC is the integral value of the contrast intensity at each time point to the contrast time, reflecting the cumulative perfusion intensity during the whole contrast period. A: control group, B: model control group, C: cavitation group, D: high dose colchicine group, E: cavitation + low dose colchicine group, F: cavitation + high dose colchicine group.

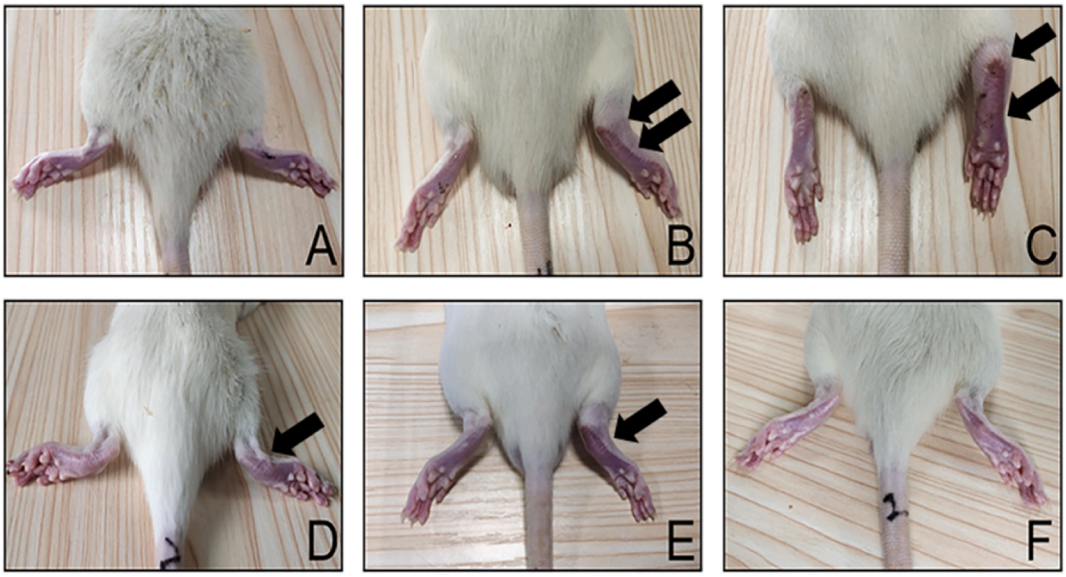

Fig. 5. Swelling of the ankle joint of rats in each group 24 h after injection of MSU.
A: No obvious redness and swelling of the ankle joint; B: Obvious redness and swelling of the ankle joint; C: Obvious redness and swelling of the ankle joint; D: Swelling and dark color of the ankle joint; E: visible swelling of the ankle joint with dark color; F: No obvious redness or swelling was observed in the ankle (black arrows indicate obvious swelling in the rat ankle, and the number of arrows indicates the degree of swelling). A: control group, B: model control group, C: cavitation group, D: high dose colchicine group, E: cavitation + low dose colchicine group, F: cavitation + high dose colchicine group.

Table 2
Comparison of gait scores and gastrointestinal reactions scores between groups [$(\overline{x} \pm s)/M(Q_1,Q_3)$].

Group	gait score	gastrointestinal reactions scores
A	0(0,1.00)	0(0,1.00)
B	2.60 ± 0.55^{a}	0(0,1.00)
C	2.40 ± 0.89^{a}	0(0,1.00)
D	$0.50(0,0.50)^{abc}$	$2.00(1.00,2.00)^{abc}$
E	$0.50(0,1.00)^{abc}$	$0.50(0,0.50)^{abcd}$
F	$0(0,1.00)^{bcde}$	$2.00(1.00,2.00)^{abce}$
H	20.575	20.961
P	<0.001	<0.001

Compared with group A, $^{a}P < 0.05$; Compared with group B, $^{b}P < 0.05$; Compared with group C, $^{c}P < 0.05$; Compared with group D, $^{d}P < 0.05$; Compared with group E, $^{e}P < 0.05$.

0.05). The analysis of IL-1β and eNOS between groups is shown in Table 1.

3.5. Effect of USMB combined with colchicine on inflammatory infiltration of the ankle joint in AGA

Hematoxylin-eosin (HE) staining revealed that the synovial tissue morphology and structure in group A were relatively preserved, with no significant histopathological alterations observed. In contrast, groups B and C exhibited marked synovial tissue damage, characterized by necrosis, edema, hemorrhage, and an influx of inflammatory neutrophils into the synovial tissue. The extent of joint damage in groups D, E, and F was less pronounced than that in group B, with group D showing similar damage to group E, but greater than that observed in group F. Additionally, mast cells were noted in the HE-stained sections of group F. The comparative HE staining results of ankle joints across the groups are depicted in Fig. 6(A–F).

3.6. Effect of USMB combined with colchicine on gastrointestinal response scores in rats

There was no significant difference among groups A, B and C, and the scores of gastrointestinal reaction were lower than those in groups D, E and F ($P < 0.05$). Compared with group D, the gastrointestinal scores in group E were significantly lower ($P < 0.05$), and there was no significant difference in group F ($P > 0.05$). Compared with group E, the gastrointestinal reaction score of group F was higher ($P < 0.05$). The analysis of gastrointestinal reaction between groups is shown in Table 2.

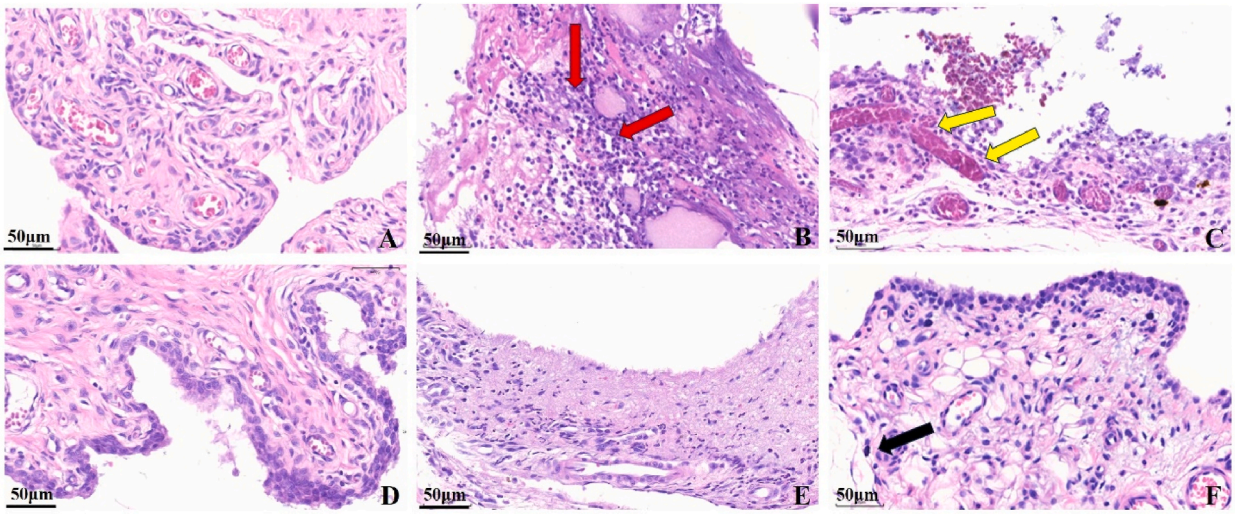

Fig. 6. HE staining of pathological sections of ankle joint in each group.
In group A, which functioned as the control group, the synovial tissue manifested a regular morphology and intact structure, devoid of any overt histopathological anomalies upon microscopic inspection. Group B, designated as the model control group, presented a severely disrupted synovial tissue architecture. The structural integrity was compromised, accompanied by prominent synovial necrosis, extensive edema, and visible hemorrhage. Moreover, a dense infiltration of inflammatory neutrophils was detected, signifying an intense inflammatory reaction within the tissue.
Group C, identified as the cavitation group, also exhibited a markedly damaged synovial tissue structure. The synovium was ravaged by necrosis, swollen due to edema, and marred by bleeding. Concurrently, a significant influx of inflammatory neutrophils was observed. Group D, labeled as the high-dose colchicine group, the synovial tissue surface was found to be irregular. Scattered neutrophil infiltrations were discernible within the tissue. In group E, termed the cavitation + low-dose colchicine group, the synovial tissue surface was likewise uneven, and there was less neutrophil infiltration in the synovial tissue.
Group F, the cavitation + high-dose colchicine group, boasted a relatively intact synovium. Although occasional exfoliation of epithelial cells and telangiectasia were observable, the frequency of neutrophil infiltration was minimal. The red arrow shows neutrophil infiltration; The yellow arrows indicate synovial bleeding; The black arrows show mast cells.

4. Discussion

The present study endeavors to investigate the effects of the combination of colchicine and USMB by employing a rat model of AGA. The experimental outcomes revealed a remarkable boost in blood perfusion within AGA-afflicted rats when colchicine was paired with USMB. In contrast to the administration of colchicine alone, the combination regimen not only curbed inflammatory responses more effectively but also translated into tangible improvements in the clinical manifestations of AGA. Specifically, there was a notable reduction in ankle joint swelling and gait abnormalities, which are key indicators of disease severity. Concurrently, the levels of plasma IL-1β dropped, and the infiltration of neutrophils in the synovial membrane was mitigated, attesting to the anti-inflammatory potency of the combined treatment. Evidently, these results spotlight the enhanced therapeutic effectiveness of integrating colchicine with USMB. Of particular interest is the discovery that, with the assistance of USMB, a reduced dosage of colchicine could still yield favorable outcomes in treating AGA in rats, while simultaneously minimizing the occurrence and severity of gastrointestinal side effects. This further emphasizes the potential of the colchicine-USMB combination as a viable and efficient therapeutic strategy for combating AGA, holding promise for future clinical applications and research directions.

The application of finely tuned ultrasonic parameters, including MI and repetitive pulse frequency, facilitated the generation of low-energy steady-state cavitation. This manipulation resulted in an enhancement of blood perfusion within the ankle joint of rats. The primary blood supply to the rat ankle joint, which is derived from the anterior tibial artery and its intricate network of smaller branches, is relatively limited compared to organs with more abundant blood flow, thereby impeding the efficient delivery of therapeutic agents such as colchicine to the affected synovium Jung et al. have confirmed that the area AUC value, obtained through CEUS, can quantitatively analyze tissue blood perfusion. In this study, the AUC value was employed to analyze blood perfusion in the rat ankle joint with high precision. The induction of steady-state cavitation through ultrasound stimulation of microbubbles has been demonstrated to augment blood perfusion in portions of tumors [14]. The manipulation of ultrasonic parameters, specifically the MI and repetitive pulse frequency, enabled the generation of low-energy steady-state cavitation, which in turn facilitated enhanced drug penetration and bolstered the therapeutic efficacy of colchicine. Following cavitation, there was an observed increase in blood perfusion within the ankle joint of rats, a phenomenon that could potentially elevate local drug concentrations. The primary blood supply to the rat ankle joint, which includes the anterior tibial artery and its intricate network of smaller branches, is relatively limited compared to organs with more abundant blood flow, thus impeding the efficient delivery of therapeutic agents such as colchicine to the affected synovium. The AUC value, derived from CEUS, has been established as a quantitative measure of tissue blood perfusion, and in this study, it was employed with high precision to analyze blood perfusion in the rat ankle joint. The introduction of steady-state

cavitation, induced by the ultrasound stimulation of microbubbles, has been demonstrated to enhance blood perfusion in parts of tumors, suggesting a similar mechanism may be at play in enhancing drug delivery to the ankle joint [15], also consistent with the findings reported by Feng et al. [16]. The underlying mechanism is likely attributed to the periodic oscillation of the cavitation nucleus, which consists of microbubbles from contrast agents, under conditions of low MI. This oscillation induces a reciprocal pushing and pulling effect, as well as acoustic radiation pressure or microflow, exerted upon the microvessels within the tissue. Consequently, this leads to aseptic inflammatory reactions that result in the localized dilation of microvessels, facilitated by vasodilator substances such as Nitric Oxide (NO) [17].

Perfluorobutane microspheres being a novel type of ultrasound contrast agent, consists of hydrogenated lecithin serine membrane-coated perfluorobutane microspheres. Perfluorobutane microspheres were first introduced into Japan as a contrast agent in 2007. Perfluorobutane microspheres garners increasing attention due to its cell surface liposome-mimicking shell structure that facilitates engulfment by Kupffer cells [18]. Our research team selected perfluorobutane microspheres as the pivotal element for cavitation, leveraging their inherent stability attributes. The high density, low diffusivity, and low saturation constant of Sonazoid endow a more sustained circulation of microbubbles in vivo. Previous studies have demonstrated that perfluorobutane microspheres reach their peak intensity at a MI of 0.4, with rupture occurring when the MI surpasses this threshold, highlighting the stability of their properties. In contrast, sulfur hexafluoride microbubbles initiate rupture at an approximate MI of 0.16 [19]. To mitigate excessive microbubble destruction during ultrasound irradiation, we opted for perfluorobutane microspheres as the cavitation nucleus, employing a MI of approximately 0.3 during irradiation adjustments. This MI is below the threshold typically associated with perfluorobutane microspheres destruction, thus achieving a state of steady-state cavitation and vasodilation. Furthermore, another study has utilized Sonazoid as a cavitation core to induce transient cavitation of microbubbles under high MI conditions, leading to targeted drug release, enhanced immune response, increased endothelial cell permeability, and improved efficacy of tumor drug treatment [20]. Eikrem et al. [21], in their comparative analysis of SonoVue and Sonazoid as cavitation nuclei, they achieved doxorubicin concentrations of 97.9 pmol/g and 111.8 pmol/g, respectively, in the kidneys of mice on the ninth day following a single drug administration. These concentrations significantly surpassed the 18.9 pmol/g obtained with doxorubicin alone, highlighting the enhanced drug delivery facilitated by these microbubbles.

Colchicine, a drug used in the clinical treatment of AGA, is an antimitotic agent that binds tubulin and inhibits microtubule polymerization [22]. The binding interaction under investigation exerts an inhibitory effect on the chemotaxis, adhesion, and phagocytic activity of neutrophils, culminating in the suppression of leukotriene and prostaglandin release, key inflammatory mediators. Consequently, this intervention effectively modulates the acute inflammatory response within the synovial joints [23]. The therapeutic dose of colchicine is perilously close to its toxic dose [24]. In this study, the concomitant administration of USMB and colchicine resulted in a significant elevation of blood perfusion within the ankle joints of rats when compared to colchicine monotherapy. This enhancement in perfusion is posited to amplify the anti-inflammatory potency of colchicine. The pharmacokinetics of colchicine revealed a peak serum concentration 1–2 h post intragastric administration, followed by a gradual decline.

The initiation of blood cell infiltration post-MSU injection coincided with a concomitant increase in IL-1β levels. eNOS, an enzyme predominantly localized within the endoplasmic reticulum of endothelial cells, exerts its biochemical activity therein [25]. NO plays a multitude of physiological roles, including the facilitation of vasodilation, the inhibition of platelet aggregation, and the exertion of anti-inflammatory effects. Within the vasculature, eNOS orchestrates the synthesis and release of NO, which induces the relaxation of vascular smooth muscle cells, leading to vasodilation. Consequently, eNOS acts as a critical modulator of vascular tone and the dynamics of blood flow [26]. Furthermore, under cavitation conditions, the dosage of colchicine can be reduced to achieve the therapeutic effect of high-dose colchicine, thus significantly reducing its side effects. Hence, denoting this combination therapy as a prospective novel intervention.

This study has some limitations. Initial investigations are confined to animal models, with the transition to human clinical trials yet to be realized. A substantial corpus of robust, evidence-based medical data is imperative to substantiate the safety and efficacy of the intervention in human subjects. Subsequent exploration is warranted to determine the optimal parameter adjustments for steady-state cavitation, thereby maximizing the enhancing effect of USMB on ankle blood perfusion. The intrinsic mechanisms underlying the vasodilation induced by steady-state cavitation are a subject that requires further elucidation in forthcoming studies.

It is noteworthy that the cavitation effect, induced by ultrasound-stimulated microbubbles, harbors substantial potential across a spectrum of applications. In this study, we exploited the characteristics of steady-state cavitation to augment targeted drug delivery by enhancing blood perfusion. As this technology advances, its integration into clinical practice is anticipated to occur progressively, thereby extending its therapeutic benefits to a broader patient population.

5. Conclusion

The synergistic administration of USMB and colchicine has been demonstrated to exert a potentiating effect on the amelioration of clinical manifestations and the enhancement of blood perfusion in rats afflicted with AGA, concurrently mitigating inflammatory markers. By leveraging USMB technology, the therapeutic efficacy akin to higher doses of colchicine can be achieved with reduced dosages, thereby diminishing the incidence of gastrointestinal adverse effects, which are commonly triggered at higher colchicine levels.

CRediT authorship contribution statement

Ji-cheng Zhang: Writing – original draft, Project administration, Methodology, Data curation. **Bo Gou:** Resources, Investigation,

Funding acquisition. **Tian-rui Wang:** Data curation. **Wan-tai Dang:** Visualization, Formal analysis. **Yan-hui Li:** Software. **Wen Wen:** Writing – review & editing, Validation. **Jian Liu:** Supervision, Funding acquisition, Conceptualization.

Data availability

The datasets used or analyzed during the current study are available from the corresponding author on reasonable request.

Research data for this article

The data that has been used is confidential.

Funding resources

Natural Science Foundation of Sichuan Province (022NSFSC0692); Medical Research Project of Sichuan Province (S23017); the First Affiliated Hospital of Chengdu Medical College (CYFYGQ18); Scientific Research Project of Chengdu Medical (2023077)

Declaration of competing interest

The authors declare that they have no known competing financial interests or personal relationships that could have appeared to influence the work reported in this paper.

References

[1] J.D. FitzGerald, N. Dalbeth, T. Mikuls, R. Brignardello-Petersen, G. Guyatt, A.M. Abeles, A.C. Gelber, L.R. Harrold, D. Khanna, C. King, et al., 2020 American College of rheumatology guideline for the management of gout, J. Arthritis Rheumatol 72 (2020) 879–895. https://www.ncbi.nlm.nih.gov/pubmed/32390306.
[2] J.A. Singh, A. Gaffo, Gout epidemiology and comorbidities, J. Semin Arthritis Rheum 50 (2020) S11–S16. https://www.ncbi.nlm.nih.gov/pubmed/32620196.
[3] M. Hui, A. Carr, S. Cameron, G. Davenport, M. Doherty, H. Forrester, W. Jenkins, K.M. Jordan, C.D. Mallen, T.M. McDonald, et al., The British society for rheumatology guideline for the management of gout, J. Rheumatol. 56 (2017) 1056–1059. https://www.ncbi.nlm.nih.gov/pubmed/28549195.
[4] J. Gao, K.A. Logan, H. Nesbitt, B. Callan, T. McKaig, M. Taylor, M. Love, A.P. McHale, D.M. Griffith, J.F. Callan, A single microbubble formulation carrying 5-fluorouridine, Irinotecan and oxaliplatin to enable FOLFIRINOX treatment of pancreatic and colon cancer using ultrasound targeted microbubble destruction, J. J Control Release 338 (2021) 358–366. https://www.ncbi.nlm.nih.gov/pubmed/34481018.
[5] J.C. Wischhusen, S.M. Chowdhury, T. Lee, H. Wang, S. Bachawal, R. Devulapally, R. Afjei, U.K. Sukumar, R. Paulmurugan, Ultrasound-mediated delivery of miRNA-122 and anti-miRNA-21 therapeutically immunomodulates murine hepatocellular carcinoma in vivo, J. J Control Release 321 (2020) 272–284. https://www.ncbi.nlm.nih.gov/pubmed/32004588.
[6] N. Li, J. Tang, J. Yang, B. Zhu, X. Wang, Y. Luo, H. Yang, F. Jang, J. Zou, Z. Liu, Z. Wang, Tumor perfusion enhancement by ultrasound stimulated microbubbles potentiates PD-L1 blockade of MC38 colon cancer in mice, J. Cancer Lett 498 (2021) 121–129. https://www.ncbi.nlm.nih.gov/pubmed/33129956.
[7] D.L. Miller, R.M. Thomas, Ultrasound contrast agents nucleate inertial cavitation in vitro, J. Ultrasound Med Biol 21 (1995) 1059–1065. https://www.ncbi.nlm.nih.gov/pubmed/8553500.
[8] B.H.A. Lammertink, C. Bos, K.M. van der Wurff-Jacobs, G. Storm, C.T. Moonen, R. Deckers, Increase of intracellular cisplatin levels and radiosensitization by ultrasound in combination with microbubbles, J. J Control Release 238 (2016) 157–165. https://www.ncbi.nlm.nih.gov/pubmed/27476609.
[9] T. Luo, L. Bai, Y. Zhang, L. Huang, H. Li, S. Gao, X. Dong, N. Li, Z. Liu, Optimal treatment occasion for ultrasound stimulated microbubbles in promoting gemcitabine delivery to VX2 tumors, J. Drug Deliv 29 (2022) 2796–2804. https://www.ncbi.nlm.nih.gov/pubmed/36047064.
[10] Y. He, X.H. Dong, Q. Zhu, Y.L. Xu, M.L. Chen, Z. Liu, Ultrasound-triggered microbubble destruction enhances the radiosensitivity of glioblastoma by inhibiting PGRMC1-mediated autophagy in vitro and in vivo, J. Mil Med Res 9 (2022) 9. https://www.ncbi.nlm.nih.gov/pubmed/35152910.
[11] C. Peng, Y. Wu, Y. Yang, N. Li, X. Chen, L. Gu, D. Xu, C. Yang, Using ultrasound-targeted microbubble destruction to enhance radiotherapy of glioblastoma, J. J Cancer Res Clin Oncol 147 (2021) 1355–1363. https://www.ncbi.nlm.nih.gov/pubmed/33547949.
[12] T.J. Coderre, P.D. Wall, Ankle joint urate arthritis in rats provides a useful tool for the evaluation of analgesic and anti-arthritic agents, J. Pharmacol Biochem Behav 29 (1988) 461–466. https://www.ncbi.nlm.nih.gov/pubmed/3362938.
[13] S.J. Lewis, K.W. Heaton, Stool form scale as a useful guide to intestinal transit time, J. Scand J Gastroenterol 32 (1997) 920–924. https://www.ncbi.nlm.nih.gov/pubmed/9299672.
[14] F. Moccetti, T. Belcik, Y. Latifi, A. Xie, K. Ozawa, E. Brown, B.P. Davidson, W. Packwood, A. Ammi, S. Huke, J.R. Lindner, Flow augmentation in the myocardium by ultrasound cavitation of microbubbles: role of shear-mediated purinergic signaling, J. J Am Soc Echocardiogr 33 (2020) 1023–1031, e1022, https://www.ncbi.nlm.nih.gov/pubmed/32532642.
[15] N. Nomikou, Y.S. Li, A.P. McHale, Ultrasound-enhanced drug dispersion through solid tumours and its possible role in aiding ultrasound-targeted cancer chemotherapy, J. Cancer Lett 288 (2010) 94–98. https://www.ncbi.nlm.nih.gov/pubmed/19674834.
[16] S. Feng, W. Qiao, J. Tang, Y. Yu, S. Gao, Z. Liu, X. Zhu, Chemotherapy augmentation using low-intensity ultrasound combined with microbubbles with different mechanical indexes in a pancreatic cancer model, J. Ultrasound Med Biol 47 (2021) 3221–3230. https://www.ncbi.nlm.nih.gov/pubmed/34362582.
[17] O.R. Mason, B.P. Davidson, P. Sheeran, M. Muller, J.M. Hodovan, J. Sutton, J. Powers, J.R. Lindner, Augmentation of tissue perfusion in patients with peripheral artery disease using microbubble cavitation, J. JACC Cardiovasc Imaging 13 (2020) 641–651. https://www.ncbi.nlm.nih.gov/pubmed/31422129.
[18] Q. Zhang, X. Liang, Y. Zhang, H. Nie, Z. Chen, A review of contrast-enhanced ultrasound using SonoVue(R) and Sonazoid in non-hepatic organs, J. Eur J Radiol 167 (2023) 111060. https://www.ncbi.nlm.nih.gov/pubmed/37657380.
[19] R.G. Barr, P. Huang, Y. Luo, X. Xie, R. Zheng, K. Yan, X. Jing, Y. Luo, H. Xu, X. Fei, J.M. Lee, Contrast-enhanced ultrasound imaging of the liver: a review of the clinical evidence for SonoVue and Sonazoid, J. Abdom Radiol (NY) 45 (2020) 3779–3788. https://www.ncbi.nlm.nih.gov/pubmed/32424608.
[20] X. Tan, C. Yi, Y. Zhang, N. Tang, Y. Xu, Z. Liu, Ultrasound-targeted microbubble destruction alleviates immunosuppression induced by CD71(+) erythroid progenitor cells and promotes PDL-1 blockade immunotherapy in the lewis lung cancer model, J. Front Oncol 11 (2021) 768222. https://www.ncbi.nlm.nih.gov/pubmed/34746009.
[21] O. Eikrem, S. Kotopoulis, M. Popa, M. Mayoral Safont, K.O. Fossan, S. Leh, L. Landolt, J. Babickova, O.A. Gudbrandsen, O.H. Gilja, et al., Ultrasound and microbubbles enhance uptake of doxorubicin in murine kidneys, J. Pharmaceutics 13 (2021). https://www.ncbi.nlm.nih.gov/pubmed/34959319.
[22] T. Pascart, P. Richette, Colchicine in gout: an update, J. Curr Pharm Des 24 (2018) 684–689. https://www.ncbi.nlm.nih.gov/pubmed/29336252.
[23] B. Goo, J. Lee, C. Park, T. Yune, Y. Park, Bee venom alleviated edema and pain in monosodium urate crystals-induced gouty arthritis in rat by inhibiting inflammation, J. Toxins 13 (2021). https://www.ncbi.nlm.nih.gov/pubmed/34564665.

[24] M. Sheibani, N. Zamani, A.H. Gerami, H. Akhondi, H. Hassanian-Moghaddam, Clinical, laboratory, and electrocardiographic findings in colchicine toxicity: 10 Years of experience, J. Front Med (Lausanne) 9 (2022) 872528. https://www.ncbi.nlm.nih.gov/pubmed/35665351.
[25] G. Yang, S.H. Yeon, H.E. Lee, H.C. Kang, Y.Y. Cho, H.S. Lee, J.Y. Lee, Suppression of NLRP3 inflammasome by oral treatment with sulforaphane alleviates acute gouty inflammation, J. Rheumatol. 57 (2018) 727–736. https://www.ncbi.nlm.nih.gov/pubmed/29340626.
[26] S.K. Kim, J.Y. Choe, K.Y. Park, Rebamipide suppresses monosodium urate crystal-induced interleukin-1beta production through regulation of oxidative stress and caspase-1 in THP-1 cells, J. Inflammation 39 (2016) 473–482. https://www.ncbi.nlm.nih.gov/pubmed/26454448.